

# PCCP

Accepted Manuscript



This is an *Accepted Manuscript*, which has been through the Royal Society of Chemistry peer review process and has been accepted for publication.

*Accepted Manuscripts* are published online shortly after acceptance, before technical editing, formatting and proof reading. Using this free service, authors can make their results available to the community, in citable form, before we publish the edited article. We will replace this *Accepted Manuscript* with the edited and formatted *Advance Article* as soon as it is available.

You can find more information about *Accepted Manuscripts* in the [Information for Authors](#).

Please note that technical editing may introduce minor changes to the text and/or graphics, which may alter content. The journal's standard [Terms & Conditions](#) and the [Ethical guidelines](#) still apply. In no event shall the Royal Society of Chemistry be held responsible for any errors or omissions in this *Accepted Manuscript* or any consequences arising from the use of any information it contains.

# N-Alkylthienopyrroledione versus Benzothiadiazole Pulling Units in Push-Pull Copolymers Used for Photovoltaic Applications: Density Functional Theory Study

Received 00th January 20xx,  
Accepted 00th January 20xx

DOI: 10.1039/x0xx00000x

www.rsc.org/

Jamin Ku,<sup>a</sup> Yeongrok Gim,<sup>a</sup> Yves Lansac<sup>b</sup> and Yun Hee Jang<sup>a,\*</sup>

Low-band-gap push-pull copolymers are promising donor materials for bulk heterojunction organic solar cells. One of the best push-pull copolymers are composed of bridged dithiophene pushing units and benzothiadiazole (BT) pulling units, but BT has no proper position to accommodate alkyl side chains introduced to enhance the solubility of resulting copolymers in organic solvents. On the other hand, N-alkylthienopyrroledione (TPD), which has an alkyl side chain attached to its pyrrole moiety, has been combined with various bridged dithiophene pushing units to give high-solubility donor polymers whose power conversion efficiencies are higher than those of the BT-based polymers especially after a morphology control. However, our well-validated time-dependent density functional theory calculation on the intrinsic (single-chain) electronic structure, which has been proved powerful to estimate the efficiency, gives a contradictory prediction that both polymers would show essentially the same efficiency. Intrigued by this, we subsequently perform density functional theory calculations on their  $\pi$ -stacked-pair models in a number of stacking configurations and conclude that the enhanced performance of the TPD-based polymers is ascribed to their enhanced inter-chain interaction resulted from their enhanced dipole moments in the push-pull direction. Enhanced morphological ordering ( $\pi$ -stacking and  $\pi$ -conjugation) in their solid films, which are not considered in electronic-structure calculations, would reduce the band gap (as proved by the low-energy shoulders in UV/vis absorption spectra), improve the charge transfer (as shown by the calculated transfer integral, transfer rate, and hole mobility), and enhance the power conversion efficiencies (as observed after a morphology control).

## 1. Introduction

Roll-to-roll mass production of organic photovoltaic (OPV) cells from low-cost light-weight flexible materials will eventually bring solar energy to interesting applications at conventional fuel costs.<sup>1</sup> Low power conversion efficiency (PCE), its major drawback, has been dramatically improved with a bulk heterojunction architecture where *push-pull*-type polymeric donors are mixed with fullerene-derivative acceptors.<sup>2-7</sup> A *push-pull* copolymer exhibits a low band gap and a strong absorption of the solar spectrum owing to the presence of both electron-rich *pushing* units and electron-deficient *pulling* units. *Push-pull* polymers used for the best OPV cells<sup>8-10</sup> have exclusively chosen benzothiadiazole (BT) derivative as *pulling* units, while their *pushing* units have been chosen from various bridged dithiophenes: cyclopentadithiophene (CPDT), dithienopyrrole (DTP), dithienosilole (DTS) (1-3; Fig. 1),<sup>4-7,11-20</sup> and so on.<sup>21-23</sup> The molecular orbital (MO) energy levels, UV/visible absorption spectra, and PCE (<6%) of such BT-based polymers 1-3 have been well described by (time-dependent) density functional theory [(TD)DFT] calculations on dimer models (~2 nm;  $n = 2$  in Fig. 1) in our previous studies.<sup>24,25</sup>

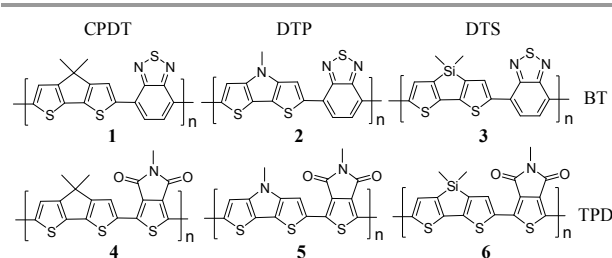


Fig. 1. Push-pull polymers 1-6 where BT (1-3) or TPD (4-6) pulling units are linked to CPDT, DTP, or DTS pushing units. All the alkyl side chains are replaced by methyl groups.

In these studies we have also designed their high-PCE derivatives where the bridging position of the dithiophene *pushing* unit [e.g. C(alkyl)<sub>2</sub> of 1] is replaced by an electron-withdrawing group such as dicyano C(CN)<sub>2</sub>, dicyanomethylene C=C(CN)<sub>2</sub>, and carbonyl C=O.<sup>24,25</sup> However, this position is where long alkyl chains are introduced to ensure the solubility of the polymer in organic solvents for solution-processed production without exerting steric hindrance against neighboring units in the same backbone and twisting it. Therefore our newly-designed polymers lacking the long alkyl side chains would be insoluble in most organic solvents, unless the long alkyl chains are introduced to the *pulling* units. Unfortunately, the current *pulling* unit, BT, has no proper position to accommodate the long alkyl chains while keeping the planarity of the backbone which is critical for good OPV characteristics.

<sup>a</sup> School of Materials Science and Engineering, Gwangju Institute of Science and Technology, Gwangju 61005, Korea

<sup>b</sup> GREMAN, UMR 7347, Université François Rabelais, 37200 Tours, France

\* Corresponding author: Yun Hee Jang (yhjang@gist.ac.kr)

Electronic Supplementary Information (ESI) available: [Experimental  $E_{\text{HOMO}}$  and  $E_{\text{g}}$  value; the Cartesian coordinates of DFT optimized structures]. See DOI: 10.1039/x0xx00000x

Hence, in order to expand the design scope of *pushing* units without sacrificing the solubility of the resulting polymers, it would be desirable to develop a *pulling* unit incorporated with long alkyl side chains. In fact, a recent development of OPV donor polymers<sup>8-10</sup> has been along this line, introducing alkylated *pulling* units such as N-alkylthienopyrroledione (TPD),<sup>26-48</sup> alkylthienothiophene,<sup>49,50</sup> bis-N-alkyldiketopyrrolopyrrole,<sup>51</sup> and 2-alkylbenzotriazole.<sup>52-55</sup> [2,2-Dialkylbenzimidazole with C(alkyl)<sub>2</sub> at the position of S of BT has also been proposed but it turned out to go through a degradation under a conventional polymer synthesis condition.<sup>56</sup>] Among them, TPD has been combined with the same bridged dithiophene *pushing* units (CPDT, DTP, and DTS) as in **1-3** to make highly-soluble donor polymers **4-6** (Fig. 1).<sup>29-40</sup> Their PCE's have been measured up to 7.3%, which are even higher than those of **1-3**.

In this work we carry out DFT/TDDFT calculations on the single-chain dimer models of **4-6** ( $n = 2$ , Fig. 1) in the same manner as done on **1-3** in our previous study<sup>24</sup> (but including the solvent effect in the current study), expecting more favorable backbone structure, electronic structure, optical properties, and PCE values for **4-6** than for **1-3**. Our calculation scheme has been carefully validated against various polymers of such kind and proved reliable for predicting PCE,<sup>24,25,56,57</sup> but we are surprised to find essentially the same electronic structure and PCE predicted for both classes of polymers in contrast to the observation (Sections 2.1 and 3.1). Intrigued by this discrepancy, we subsequently perform DFT calculations on their  $\pi$ -stack-paired monomer models ( $n = 1$ , Fig. 1) and conclude that the enhanced performance of the TPD-based polymers **4-6** is ascribed to their enhanced inter-chain interaction (stronger binding in the  $\pi$ -stacked pair) resulting from their enhanced dipole moments in the *push-pull* direction (Sections 2.2 and 3.2).

## 2. Calculation Details

**2.1. Single-chain models.** The same type of calculation as done in our previous studies<sup>24,25,56,57</sup> is carried out using *Jaguar v6.5*<sup>58,59</sup> and *Gaussian09*.<sup>60</sup> The optimized structures of the monomer and dimer models of BT-based **1-3** are taken from our previous study<sup>24</sup> to build the monomer and dimer models of the TPD-based **4-6** ( $n = 1-2$ ; Fig. 1). All the alkyl side chains are replaced by methyl groups to simplify the calculation (Fig. 1). The ground-state geometry is fully optimized at the B3LYP<sup>61-65</sup>/6-311G(d,p) level in the gas phase and in the CHCl<sub>3</sub> (chloroform) solution using the CPCM (conductor-like polarizable continuum model) implicit solvent model.<sup>66,67</sup> The energy levels of the highest occupied molecular orbitals (HOMO),  $E_{\text{HOMO}}$ , are taken from the eigenvalues of the Kohn-Sham equation. The first ionization potential [=  $E(\text{cation}) - E(\text{neutral})$ ] should in principle be more appropriate to compare with experimental  $E_{\text{HOMO}}$ , which is estimated electrochemically from the oxidation onset potential,<sup>68</sup> but inspection of previous studies including ours<sup>24</sup> indicates that our approach is as simple and reliable (requiring only dimer models instead of tetramer for closer agreement with experiments). At the optimized geometry, the vertical singlet-singlet electronic transition energies are calculated with the TDDFT method<sup>69-72</sup> at the same level of theory. The UV/vis absorption spectra are simulated on the basis of the TDDFT calculations, employing Gaussian functions with a fixed width of 0.4 eV to build a continuous spectrum from a collection of transition peaks corresponding to the TDDFT transition

energies and oscillator strengths. The lowest ( $S_0 \rightarrow S_1$ ) vertical transition energy gives the optical band gap ( $E_g$ ; eV) corresponds to the lowest peak maximum  $\lambda_{\text{max}}$  (not the onset  $\lambda_{\text{onset}}$ ; nm) in the absorption spectrum ( $E_g = 1240 / \lambda_{\text{max}}$ ). Our band gap  $E_g$  should be compared with literature values with care, because the optical band gaps in literature (ref. 68, for example) are typically much lower values converted from the absorption onset wavelengths  $\lambda_{\text{onset}}$ . Since most (~90%) of the lowest-energy ( $S_0 \rightarrow S_1$ ) transition in most copolymers of the same type (ref. 68, for example) comes from the electronic transition from HOMO to the lowest unoccupied molecular orbitals (LUMO), the lowest TDDFT transition energy can be approximated as the HOMO-LUMO energy gap and thus the energy levels of the lowest unoccupied molecular orbitals (LUMO),  $E_{\text{LUMO}}$ , are approximately estimated by adding  $E_{\text{HOMO}}$  of DFT and the transition energies of TDDFT [ $E_{\text{LUMO}} = E_{\text{HOMO}}(\text{DFT}) + E_g(\text{TDDFT})$ ].

**2.2. Stack-paired models.** The strength of inter-chain interaction is estimated from the binding energy (BE) between two monomer models ( $n = 1$ ; Fig. 1) in a  $\pi$ -stacked pair [BE =  $2 \times E(\text{isolated monomer}) - E(\pi\text{-stacked pair})$ ]. Numerous initial configurations of a  $\pi$ -stacked pair are generated by systematically changing the distance, angle, and orientation of the second monomer with respect to the first one and then submitted to a full geometry optimization in the gas phase at the  $\omega\text{B97XD}/6\text{-311G(d,p)}$  level of DFT. The  $\omega\text{B97XD}$  functional ( $\omega\text{B97X}$ <sup>73-75</sup> combined with the Grimme's dispersion correction<sup>76,77</sup>) is known as *probably the most recommendable DFT-based method for non-covalent complexes*, which avoids the underbinding (B3LYP) and overbinding (B3LYP-D) problems.<sup>78</sup> Since *most DFT-D schemes are parameterized without employing the counterpoise correction of the basis set superposition error and should be used this way with at least triple-zeta quality basis sets*,<sup>78</sup> we also skip the counterpoise correction in this study.

## 3. Results and discussion

**3.1. Single-chain models.** The dihedral energy curves of **1-6**, that is, the energy changes as a function of the dihedral angle between the pushing and pulling units (SCCC<sub>H</sub> for **1-3** and SCCS for **4-6**; Fig. 2) indicate that the minimum-energy structures of **1-6** have a planar backbone conformation with a dihedral angle around 0°. This planar conformation is 2-3 kcal/mol more stable than the other planar conformation with a dihedral angle around 180° and well separated from it by a barrier of 6-7 kcal/mol. Hence the following analyses are performed on this conformation as done in previous DFT studies<sup>40,48,79</sup> [contrary to other DFT studies<sup>29,39,80</sup> which assume the latter conformation with the S---O bond as a conformational lock].

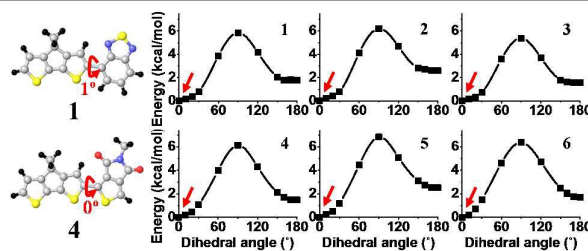


Fig. 2. Dihedral energy curves of the monomer models of **1-6**. The minimum-energy structure indicated by red arrows is shown for **1** and **4**. Color code: black (H), gray (C), blue (N), red (O), and yellow (S).

The HOMO energy levels ( $E_{\text{HOMO}}$ ) from the DFT calculations on the dimer models of **1-6** in  $\text{CHCl}_3$  are shown in Table 1 and Fig. 3a (red marks) along with a collection of the experimental values from the cyclic voltammetry (CV; black bars).<sup>4,5,7,14,16-19,29-35,37-40,81,82</sup> [Some values for **6**,<sup>35,37</sup> which were converted from the oxidation onset potential ( $E_{\text{ox}}$ ) using a different formula ( $E_{\text{HOMO}} = -E_{\text{ox}} - 5.12$  eV) from the one used for all the others ( $E_{\text{HOMO}} = -E_{\text{ox}} - 4.8$  eV),<sup>83,84</sup> are excluded from the comparison.] The calculated  $E_{\text{HOMO}}$ 's of all the polymers **1-6** fall within the range of the experimental values. The  $E_{\text{HOMO}}$ 's of **4-6** are slightly lower than those of **1-3**, most likely due to  $E_{\text{HOMO}}$  of TPD itself (-7.50 eV) which is lower than that of BT (-6.84 eV), indicating that the TPD-based donor polymers **4-6** would show larger open-circuit voltages  $V_{\text{oc}} [= E_{\text{LUMO}}(\text{acceptor}) - E_{\text{HOMO}}(\text{donor})]$  (favorably for PCE) than the BT-based **1-3**. The  $E_{\text{HOMO}}$ 's of **1-3** and **4-6** follow the same pattern: an electron-withdrawing character of the bridging position of the dithiophene pushing unit [N(alkyl) < C(alkyl)<sub>2</sub> < Si(alkyl)<sub>2</sub>] pulls down  $E_{\text{HOMO}}$  (**2** > **1** > **3** and **5** > **4** > **6**).

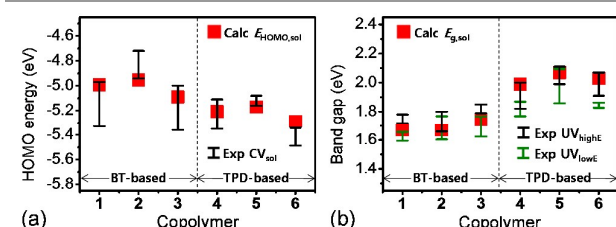


Fig. 3. (a) HOMO energy levels and (b) band gaps of the dimer models of **1-6** in  $\text{CHCl}_3$  (red mark; this work) and the corresponding experimental data (the oxidation onset potential in CV and the first peak maximum in UV/vis absorption spectra (black and green bars; see Table 1 for data; see text for references).

Table 1. HOMO energy levels and band gaps of **1-6**.

	$-E_{\text{HOMO}}$ (eV)		$E_{\text{g}}$ (eV/nm)		
	calc <sup>a</sup>	exp (CV) <sup>b</sup>	calc <sup>c</sup>	exp ( $\lambda_{\text{max}}$ ) <sup>d</sup>	exp ( $\lambda_{\text{max}}$ ) <sup>e</sup>
<b>1</b>	4.99	4.9-5.33	1.67 (741)	1.70-1.80 (690-730)	1.60-1.65 (750-775)
<b>2</b>	4.95	4.65-4.94	1.67 (742)	1.62-1.82 (684-765)	1.60-1.76 (706-777)
<b>3</b>	5.09	5.05-5.36	1.74 (713)	1.77-1.85 (670-700)	1.57-1.80 (690-790)
<b>4</b>	5.21	5.08-5.43	1.99 (622)	1.76-2.05 (604-705)	1.77-1.85 (671-701)
<b>5</b>	5.17	5.09-5.16	2.07 (600)	1.92-2.11 (588-645)	1.81-2.07 (598-686)
<b>6</b>	5.29	5.33-5.52	2.03 (612)	1.84-2.04 (608-673)	1.85-1.86 (665-671)

<sup>a</sup>From DFT in  $\text{CHCl}_3$  (this work). <sup>b</sup>From the oxidation onset potentials (see text for references). <sup>c</sup>From TDDFT in  $\text{CHCl}_3$  (this work). <sup>d,e</sup>From the first peak maximum at high- and low-energy shoulders of thin-film UV/vis absorption (Fig. 4; see text for references).

The band gaps ( $E_{\text{g}}$ ) estimated from the lowest TDDFT transition energies of **1-6** in  $\text{CHCl}_3$  are summarized in Table 1 and Fig. 3b (red marks). The UV/vis absorption spectra of **1-6** simulated from the TDDFT transition energies and oscillator strengths are shown in Fig. 4 (black peaks and curves). Shown together is a collection of the experimental spectra (color curves) measured in solutions (Fig. 4a) and in solid thin films (Fig. 4b). The experimental spectra (of **4** and **6** in particular) exhibit a solution-to-film bathochromic red shift due to a development of low-energy shoulders on the first absorption peaks measured on thin films. Such low-energy shoulder peaks are often observed for  $\pi$ -conjugated polymers with a strong inter-chain

interaction as a signature of  $\pi$ -stacked polymer crystalline phases with extended conjugation lengths.<sup>4,30-32,39,85</sup> The experimental  $E_{\text{g}}$  estimated from the position of such high- and low-energy shoulders (*intrinsic*  $E_{\text{g}}$  of a polymer chain versus *thin-film*  $E_{\text{g}}$  of a  $\pi$ -stacked phase) is summarized in Fig. 3b (black versus green bars) and Table 1.<sup>4,5,7,11,12,14,16-19,29-35,37-40,82,86-91</sup> The solution-to-film red shift due to the low-energy shoulder is more prominent for **4-6** than **1-3** (Fig. 4), implying that the TPD-based **4-6** have a higher tendency to form  $\pi$ -stacks than the BT-based **1-3**. Indeed, the TDDFT absorption spectra (black curves, Fig. 4) and  $E_{\text{g}}$  (red marks, Fig. 3b) calculated on the single-chain models are in a good agreement with those measured for **1-3** (colored curves, Fig. 4; black and green bars, Fig. 3b) and also with the *intrinsic* characteristics of **4-6** measured in solutions (colored curves, Fig. 4a) and films (high-energy shoulders of colored curves, Fig. 4b; black bars, Fig. 3b), but fail to reproduce the *thin-film* characteristics of **4-6** (low-energy shoulders of colored curves, Fig. 4b) and significantly overestimate the *thin-film*  $E_{\text{g}}$  of **4-6** (green bars, Fig. 3b). A greater amount of  $\pi$ -stacked aggregates in their films is expected for **4-6** than for **1-3**.

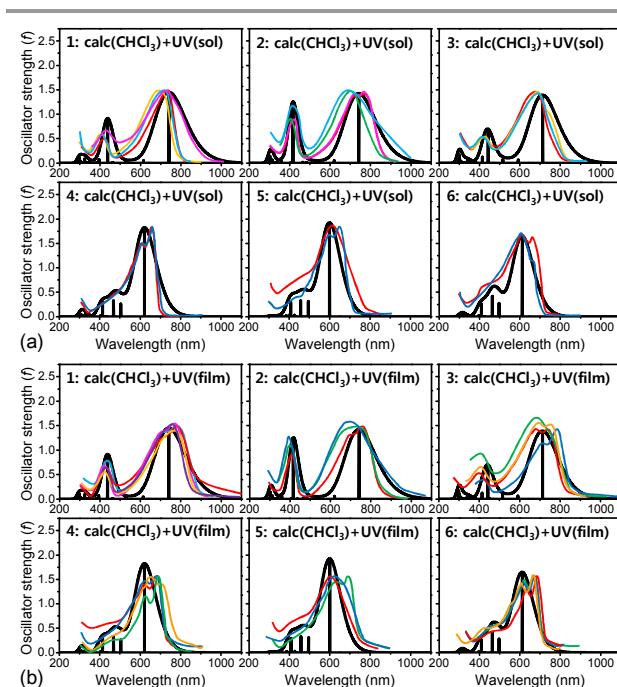


Fig. 4. TDDFT absorption spectra of the dimer models of **1-6** in  $\text{CHCl}_3$  (black peaks and curves; this work) and experimental UV/vis absorption spectra (colored curves; see text for references) measured in solutions (a) and on thin films (b).

The TPD-based **4-6** show significantly larger  $E_{\text{g}}$  (unfavorably for PCE) than the BT-based **1-3** (because TPD itself has a wider  $E_{\text{g}}$  than BT; 4.54 versus 3.87 eV) and slightly lower  $E_{\text{HOMO}}$  (favorably for PCE) for **4-6** than for **1-3**, and thus  $E_{\text{LUMO}} (= E_{\text{HOMO}} + \textit{intrinsic} E_{\text{g}})$  is higher (unfavorably for PCE)<sup>24</sup> for **4-6** than for **1-3** (Fig. 5a). The PCE values (in %) evaluated by plugging the *intrinsic*  $E_{\text{g}}$  and  $E_{\text{LUMO}}$  into the Scharber diagram<sup>92-94</sup> as done in our previous studies<sup>24,25,56</sup> are thus essentially the same for both **1-3** (3.9, 3.3, and 4.2; yellow mark, Fig. 5b; blue squares, Fig. 5c) and **4-6** (3.9, 3.2, and 4.1; red marks, Fig. 5b; blue squares, Fig. 5c). The PCE's estimated for **1-3** from their *intrinsic* electronic structure calculated in  $\text{CHCl}_3$  are higher than

those previously estimated in the gas phase (3.2, 2.4, and 3.5)<sup>24</sup> but still agree well with the experiments PCE's (black bar, Fig. 5c): 1.9–3.5 (1), 0.7–2.8 (2), and 1.2–5.2 (3).<sup>4,5,11–13,15–17,19,20,54,82,95</sup> The PCE's estimated likewise for 4–6 also agree well with the experiments: 1.0–4.9 (4), 0.6–1.9 (5), and 1.2–4.4 (6).<sup>29–34,38</sup> A morphology control with 1,8-diiodooctane (DIO)<sup>6,95,96</sup> or microwave heating,<sup>14</sup> which transforms an amorphous<sup>29,31</sup> or phase-segregated<sup>37</sup> blend film into a fine interpenetrating structure of well-ordered domains whose small sizes improve exciton dissociation, charge separation, short-circuit current, and PCE,<sup>37,39</sup> however, makes a more dramatic effect on 4–6 than on 1–3, achieving a higher PCE for 4 (<6.4)<sup>30,32</sup> and 6 (<7.3)<sup>35–39</sup> than for 1 (<5.5)<sup>6,15,95</sup> and 3 (<5.9),<sup>14</sup> again indicating that the TPD-based polymers, 4 and 6 in particular, have stronger  $\pi$ -stacking interchain interaction than the BT-based ones, but this effect is not included in our single-chain-based PCE estimation.

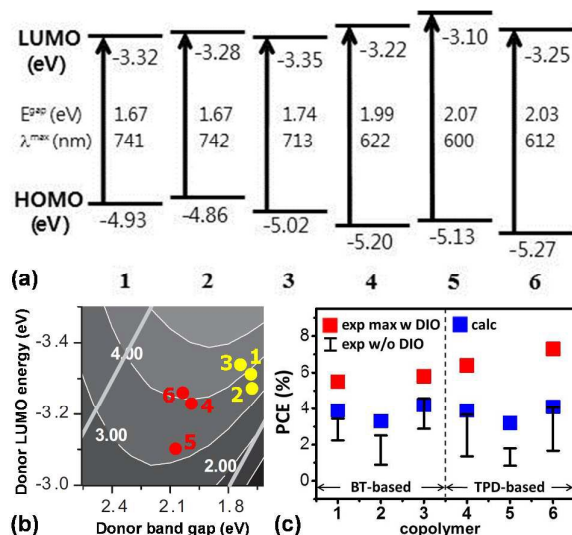


Fig. 5. (a) Frontier MO diagram of the dimer models of 1–6 in  $\text{CHCl}_3$ , where the vertical arrows indicate the  $S_0 \rightarrow S_1$  transitions whose principal contributions come from the HOMO  $\rightarrow$  LUMO transitions, (b) the Scherbar diagram to estimate the PCE of the OPV cells containing 1–3 (yellow circle) and 4–6 (red circle), and (c) the calculated (blue square) and experimental [with and without 1,8-diiodooctane (DIO); black bar and red square] PCE values (see text for references).

**3.2. Stack-paired models.** A pair of two monomer models is taken as the simplest model describing the inter-chain interaction which is a rather localized and short-range quantity. From a full geometry optimization starting from a number of initial pairing configurations, seven distinct configurations of the strongest binding are selected and presented in Fig. 6. They are all *face-on*  $\pi$ -stacked pairs, as suggested from experiments.<sup>31,37,39</sup> In these seven configurations, two monomer models face each other in the same orientation (FF), with one monomer flipped about the short axis (x) (FFX) or the long axis (y) (FFY) or both (FFZ), or in a cross form (CF). They can also be significantly shifted from each other (FFXS or FFYS). The inter-planar  $\pi$ -stacking distance is calculated as  $\sim 3.6$  Å, which is close to the value estimated from a grazing incidence wide-angle x-ray scattering experiment (3.7 Å).<sup>39</sup> As expected from all the discussions above, the seven most strongly bound pairs of 4 have indeed overall higher binding energies (BE; 24.3, 24.0, 23.9, 23.8, 22.0, 21.5, and 19.9 kcal/mol; Fig. 6, right) than those of 1 (22.3, 22.1, 22.0, 20.9, 20.1, 20.1, and 17.5 kcal/mol, Fig. 6, left). [A simple

test with one configuration (FFY) of stacked-pair dimer models (not shown here) gives a binding energy of 21.6 (1) and 23.6 (4) kcal/mol per monomer unit, which is essentially the same as those obtained with the monomer models (22.3 and 23.8 kcal/mol), confirming the validity of our simple model.]

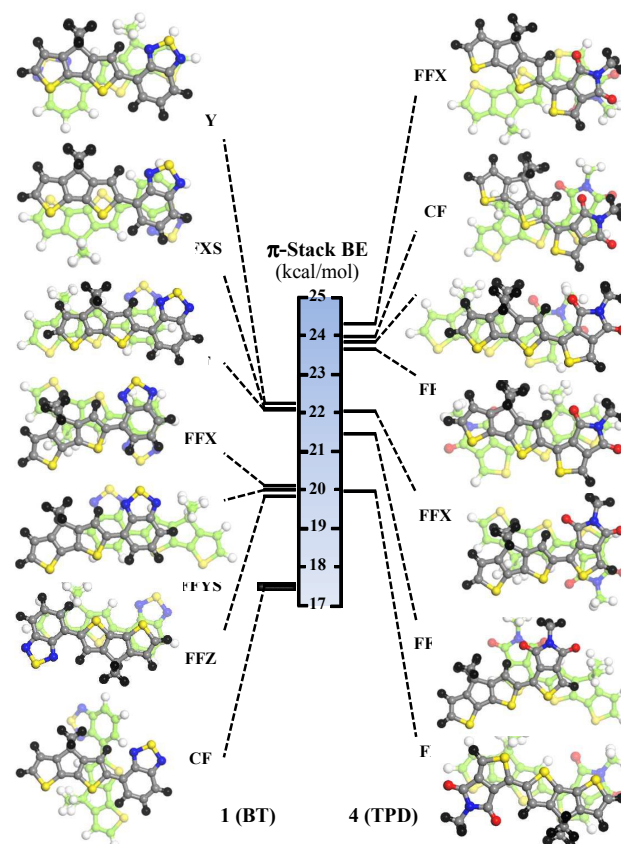


Fig. 6. Binding energy (BE) of 1 and 4 in various optimized configurations of  $\pi$ -stacked monomer pairs. Color code: gray and light green (C); black and white (H); blue and light blue (N); yellow and light yellow (S); red and light red (O).

The stronger electron-withdrawing character (the lower HOMO and LUMO energy levels) of TPD than of BT would result in a larger amount of charge separation ( $q$  in electron unit from the Mulliken population analysis) between the pushing units ( $+q$ ) and the pulling units ( $-q$ ) in 4 (0.11) than in 1 (0.03). As Fig. 7 shows, the magnitude of the dipole moment vector lying in the direction from the *pushing* unit to the *pulling* unit is larger for 4 (3.4 D) than for 1 (1.7 D). This would bring an inter-chain dipole-dipole interaction in addition to the  $\pi$ - $\pi$  interaction, and it would be stronger for 4 than for 1.

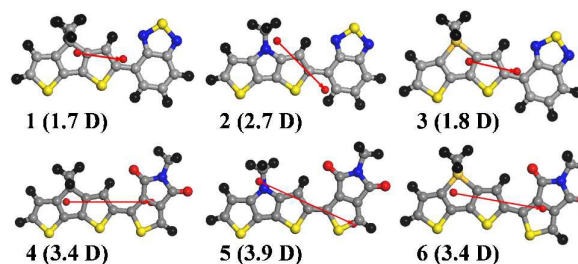


Fig. 7. Dipole moment vectors developed in the push-pull direction of 1–6.

As will be reported in detail separately in near future, the hole transport properties (hole transfer integrals, hole transfer rates and hole mobilities) of **1** and **4** are evaluated on the seven stacked-pair configurations following previous studies<sup>80,97,98</sup> and Boltzmann-averaged on the basis of the relative BE with respect to the lowest-energy configuration. The average hole transfer integral, hole transfer rate and hole mobility of **4** are indeed higher (by 20-50%) than those of **1**, explaining in part the difference in PCE between **1** (<5.5%)<sup>6,15,95</sup> and **4** (<6.4%)<sup>30,32</sup> after a morphology control.

The difference in the inter-chain interaction between **1** and **4** would be even larger in reality when all the long alkyl side chains (two of the pushing units and one of the TPD pulling unit in **4** and two of the pushing unit in **1**) are introduced to the positions of the methyl groups and contribute to inter-chain dispersion interaction. Among the series of **4-6** (and **1-3**), the copolymer with the DTP pushing unit, **5** (and **2**), have the largest dipole moment 3.9 D (and 2.7 D) due to the most electron-donating (*pushing*) character of the bridging N(alkyl) in DTP (Fig. 7) and would exert the strongest dipole-dipole inter-chain interaction. However, only two long alkyl chains would be present in **5**, instead of three present in **4** and **6** (and only one in **2** instead of two in **1** and **3**), exerting the weakest alkyl-alkyl dispersion interaction. The two effects would cancel each other and thus would not alter the sequence of PCE estimated from their intrinsic electronic structure ( $6 \sim 4 > 5$  and  $3 \sim 1 > 2$ ).

**3.3. Proposition.** The same sequence of PCE's is predicted for both series of polymers ( $6 \sim 4 > 5$  and  $3 \sim 1 > 2$ ). We thus expect that the same type of PCE enhancement as proposed for the BT-based polymers in our previous studies (up to 6-11%)<sup>12,13</sup> could be proposed for the TPD-based polymers (**7-12**, Fig. 8).<sup>24,25</sup> A realization of our previous proposition for the BT-based polymers has not been reported yet, probably due to their low solubility with a limited number of long alkyl side chains (zero in the BT-analogues of **7-9** and one in the BT-analogues of **10-12**), but the situation should be improved by replacing BT with N-alkylated TPD (one long alkyl side chain in **7-9** and two in **10-12**). Therefore, we propose a potential high-performance high-solubility push-pull-type OPV donor polymer such as **7-13**, where TPD pulling units are linked to pushing units of dithiophenes bridged with various electron-withdrawing groups. The copolymer **8** and its imine derivatives **13** are particularly interesting: their analogues have been synthesized but bulky alkoxy<sup>99</sup> and alkyl<sup>100</sup> substituents introduced to ensure sufficient solubility appear to twist the backbone,<sup>25,57</sup> increase the band gap, and lower the PCE. Introducing N-alkyl-TPD units and removing those bulky substituents would improve their OPV characteristics. We hope that this proposition would call for an attention of experimentalists.

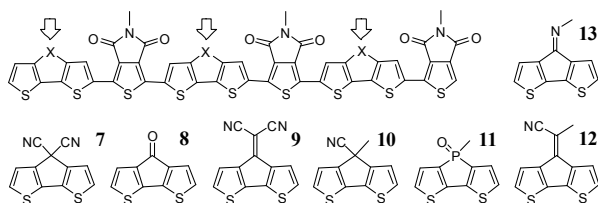


Fig. 8. Push-pull polymers **7-13** where TPD pulling units are linked to pushing units of dithiophenes bridged with electron-withdrawing groups.

## 4. Conclusions

The DFT and TDDFT calculations were carried out on push-pull OPV donor polymers composed of bridged dithiophene pushing units and TPD pulling units. The MO energy levels, band gaps and absorption spectra calculated with the solvent effect included reproduce very well the experiments except the low-energy shoulders observed on thin-film UV/vis spectra, indicating a facile formation of local  $\pi$ -stacked phases. Indeed the inter-chain interaction was calculated to be stronger in the TPD-based copolymers than in their BT analogues, probably due to its higher degree of local dipole moments developed in the charge-separated push-pull direction. A rather strong dipole-dipole interaction in addition to a  $\pi$ - $\pi$  interaction between different polymer chains (or their segments) would help inter-chain stacking and (locally) crystalline ordering. The TPD-based copolymers have lower HOMO energy levels but larger band gaps than their BT analogues, and thus a similar PCE is estimated for both polymers. The PCE measured after morphology control is slightly higher for TPD-based polymers, probably due to their stronger inter-chain interaction. We hence make the same proposition as done for the BT-based polymers in our previous study: a push-pull polymer made of TPD (pulling unit) and dithiophenes bridged with electron-withdrawing groups (pushing unit) could be a potential high-PCE high-solubility OPV donor copolymer. Another proposition we make from this work is that, contrary to a concern about the accuracy of TD-B3LYP in describing a long-range charge-transfer excitation,<sup>101-103</sup> a good agreement with experimental UV/vis absorption spectra was obtained with our simple TD-B3LYP calculations on dimer models ( $\sim 2$  nm, a typical  $\pi$ -conjugation length). Our preliminary TDDFT calculations performed with long-range-corrected functionals such as LC-BLYP,<sup>104</sup> CAM-B3LYP,<sup>105</sup> and  $\omega$ B97XD<sup>73-77</sup> gave a dramatic blue shift of the  $S_0 \rightarrow S_1$  transition (not shown here) as also observed previously<sup>84,103,106,107</sup> probably due to the short dimer model or the *out-of-the-box* default value for the range-separation parameter  $\omega$ ,<sup>103</sup> but even a combination of fine-tuned parameters and long oligomer models could not yield as good agreement as ours with experiments.<sup>103</sup> The success of our approach could be due to a fortunate error cancellation between the error from the B3LYP functional and the error from the short oligomer ( $\sim 2$  nm) model. However, since it has been stated that *the  $S_0 \rightarrow S_1$  transition of a BT-based polymer is essentially localized around the BT segments*,<sup>103</sup> we may not need to concern about the limitation of B3LYP in describing a long-range charge-transfer excitation. In any case, the level of theory used in this work [DFT  $E_{\text{HOMO}}$  and TDDFT  $E_g$  from B3LYP/6-311G(d,p) on short oligomer models ( $\sim 2$  nm)] appears practically suitable for studying push-pull OPV polymers (and small molecules<sup>84</sup>) with planar backbones.

## Acknowledgements

This work was supported by the Korean CCS 2020 Program (2014M1A8A1049267, 2014M1A8A1049321), the Basic Research Program (2013R1A1A3012254), the Korea-India SAVI Program (2013K2A1B9066145), and the Global Frontier Hybrid Interface Materials Program (2013M3A6B1078882) of the Korean National Research Foundation and also by the Brain Pool Program (151S-1-3-

1232) of KOFST, the Specialized Research Project and the DGIST-GIST Project of GIST as well as the Grand Challenge (KSC-2014-C3-032) and PLSI programs of KISTI.

## Notes and references

- 1 J. Nelson, *Mater. Today*, 2011, **14**, 462-470.
- 2 G. Yu, J. Gao, J. C. Hummelen, F. Wudl and A. J. Heeger, *Science*, 1995, **270**, 1789-1791.
- 3 W. Ma, C. Yang, X. Gong, K. Lee and A. J. Heeger, *Adv. Funct. Mater.*, 2005, **15**, 1617-1622.
- 4 D. Muhlbacher, M. Scharber, M. Morana, Z. Zhu, D. Waller, R. Gaudiana and C. Brabec, *Adv. Mater.*, 2006, **18**, 2884-2889.
- 5 Z. Zhu, D. Waller, R. Gaudiana, M. Morana, D. Muhlbacher, M. Scharber and C. Brabec, *Macromolecules*, 2007, **40**, 1981-1986.
- 6 J. Peet, J. Y. Kim, N. E. Coates, W. L. Ma, D. Moses, A. J. Heeger and G. C. Bazan, *Nature Mater.*, 2007, **6**, 497-500.
- 7 J. Y. Kim, K. Lee, N. E. Coates, D. Moses, T.-Q. Nguyen, M. Dante and A. J. Heeger, *Science*, 2007, **317**, 222-225.
- 8 G. Li, R. Zhu and Y. Yang, *Nature Photon.*, 2012, **6**, 153-161.
- 9 R. S. Kularatne, H. D. Magurudeniya, P. Sista, M. C. Biewer and M. C. Stefan, *J. Polym. Sci. Part A: Polym. Chem.*, 2013, **51**, 743-768.
- 10 M.-E. Ragoussi and T. Torres, *Chem. Commun.*, 2015, **51**, 3957-3972.
- 11 I. W. Hwang, C. Soci, D. Moses, Z. Zhu, D. Waller, R. Gaudiana, C. J. Brabec and A. J. Heeger, *Adv. Mater.*, 2007, **19**, 2307-2312.
- 12 I. W. Hwang, S. Cho, J. Y. Kim, K. Lee, N. Coates, D. Moses and A. J. Heeger, *J. Appl. Phys.*, 2008, **104**, 033706.
- 13 J. C. Bijleveld, M. Shahid, J. Gilot, M. M. Wienk and R. A. J. Janssen, *Adv. Funct. Mater.*, 2009, **19**, 3262-3270.
- 14 R. C. Coffin, J. Peet, J. T. Rogers and G. C. Bazan, *Nature Chem.*, 2009, **1**, 657-661.
- 15 S. Albrecht, S. Janietz, W. Schindler, J. Frisch, J. Kurpiers, J. Kniepert, S. Inal, P. Pingel, K. Fostiropoulos, N. Koch and D. Nehr, *J. Am. Chem. Soc.*, 2012, **134**, 14932-14944.
- 16 S. Zhang, Y. Guo, H. Fan, Y. Liu, H.-Y. Chen, G. Yang, X. Zhan, Y. Liu, Y. Li and Y. Yang, *J. Polym. Sci., Part A: Polym. Chem.*, 2009, **47**, 5498-5508.
- 17 W. Yue, Y. Zhao, S. Shao, H. Tian, Z. Xie, Y. Geng and F. Wang, *J. Mater. Chem.*, 2009, **19**, 2199-2206.
- 18 S. C. Price, A. C. Stuart and W. You, *Macromolecules*, 2009, **43**, 797-804.
- 19 J. Hou, H.-Y. Chen, S. Zhang, G. Li and Y. Yang, *J. Am. Chem. Soc.*, 2008, **130**, 16144-16145.
- 20 P. M. Beaujuge, H. N. Tsao, M. R. Hansen, C. M. Amb, C. Risko, J. Subbiah, K. R. Choudhury, A. Mavrinskiy, W. Pisula, J.-L. Bredas, F. So, K. Mullen and J. R. Reynolds, *J. Am. Chem. Soc.*, 2012, **134**, 8944-8957.
- 21 L. Huo, J. Hou, S. Zhang, H.-Y. Chen and Y. Yang, *Angew. Chem. Int. Ed.*, 2010, **49**, 1500-1503.
- 22 C.-C. Chen, W.-H. Chang, K. Yoshimura, K. Ohya, J. You, J. Gao, Z. Hong and Y. Yang, *Adv. Mater.*, 2014, **26**, 5670-5677.
- 23 J. Subbiah, B. Purushothaman, M. Chen, T. Qin, M. Gao, D. Vak, F. H. Scholes, X. Chen, S. E. Watkins, G. J. Wilson, A. B. Holmes, W. W. H. Wong and D. J. Jones, *Adv. Mater.*, 2015, **27**, 702-705.
- 24 J. Ku, Y. Lansac and Y. H. Jang, *J. Phys. Chem. C*, 2011, **115**, 21508-21516.
- 25 J. Ku, D. Kim, T. Ryu, E. Jung, Y. Lansac and Y. H. Jang, *Bull. Korean Chem. Soc.*, 2012, **33**, 1029-1036.
- 26 Y. Zou, A. Najari, P. Berrouard, S. Beaupre, B. R. Aich, Y. Tao and M. Leclerc, *J. Am. Chem. Soc.*, 2010, **132**, 5330-5331.
- 27 Y. Zhang, S. K. Hau, H.-L. Yip, Y. Sun, O. Acton and A. K.-Y. Jen, *Chem. Mater.*, 2010, **22**, 2696-2698.
- 28 A. Najari, S. Beaupre, P. Berrouard, Y. Zou, J.-R. Pouliot, C. Lepage-Perusse and M. Leclerc, *Adv. Funct. Mater.*, 2011, **21**, 718-728.
- 29 Y. Zhang, J. Zou, H.-L. Yip, Y. Sun, J. A. Davies, K.-S. Chen, O. Acton and A. K.-Y. Jen, *J. Mater. Chem.*, 2011, **21**, 3895-3902.
- 30 Z. Li, S.-W. Tsang, X. Du, L. Scoles, G. Robertson, Y. Zhang, F. Toll, Y. Tao, J. Lu and J. Ding, *Adv. Funct. Mater.*, 2011, **21**, 3331-3336.
- 31 X. Guo, H. Xin, F. S. Kim, A. D. T. Liyanage, S. A. Jenekhe and M. D. Watson, *Macromolecules*, 2011, **44**, 269-277.
- 32 C. M. MacNeill, E. D. Peterson, R. E. Nofle, D. L. Carroll and R. C. Coffin, *Synth. Met.*, 2011, **161**, 1137-1140.
- 33 E. Zhou, J. Cong, K. Tajima, C. Yang and K. Hashimoto, *Macromol. Chem. Phys.*, 2011, **212**, 305-310.
- 34 X. Hu, M. Shi, L. Zuo, Y. Nan, Y. Liu, L. Fu and H. Chen, *Polymer*, 2011, **52**, 2559-2564.
- 35 T.-Y. Chu, J. Lu, S. Beaupre, Y. Zhang, J.-R. Pouliot, S. Wakim, J. Zhou, M. Leclerc, Z. Li, J. Ding and Y. Tao, *J. Am. Chem. Soc.*, 2011, **133**, 4250-4253.
- 36 T.-Y. Chu, S.-W. Tsang, J. Zhou, P. G. Verly, J. Lu, S. Beaupre, M. Leclerc and Y. Tao, *Solar Energy Mater. Solar Cells*, 2012, **96**, 155-159.
- 37 C. M. Amb, S. Chen, K. R. Graham, J. Subbiah, C. E. Small, F. So and J. R. Reynolds, *J. Am. Chem. Soc.*, 2011, **133**, 10062-10065.
- 38 Y.-R. Hong, H.-K. Wong, L. C. H. Moh, H.-S. Tan and Z.-K. Chen, *Chem. Commun.*, 2011, **47**, 4920-4922.
- 39 X. Guo, N. Zhou, S. J. Lou, J. W. Hennek, R. P. Ortiz, M. R. Butler, P.-L. T. Boudreaux, J. Strzalka, P.-O. Morin, M. Leclerc, J. T. L. Navarrete, M. A. Ratner, L. X. Chen, R. P. H. Chang, A. Facchetti and T. J. Marks, *J. Am. Chem. Soc.*, 2012, **134**, 18427-18439.
- 40 Z. Lin, J. Bjorgaard, A. G. Yavuz, A. Iyer and M. E. Kose, *RSC Adv.*, 2012, **2**, 642-651.
- 41 C. E. Small, S. Chen, J. Subbiah, C. M. Amb, S.-W. Tsang, T.-H. Lai, J. R. Reynolds and F. So, *Nature Photon.*, 2012, **6**, 115-120.
- 42 E. Zhou, J. Cong, K. Tajima, C. Yang and K. Hashimoto, *J. Phys. Chem. C*, 2012, **116**, 2608-2614.
- 43 G.-Y. Chen, Y.-H. Cheng, Y.-J. Chou, M.-S. Su, C.-M. Chen and K.-H. Wei, *Chem. Commun.*, 2011, **47**, 5064-5066.
- 44 J. E. Donaghey, R. S. Ashraf, Y. Kim, Z. G. Huang, C. B. Nielsen, W. Zhang, B. Schroeder, C. R. G. Grenier, C. T. Brown, P. D'Angelo, J. Smith, S. Watkins, K. Song, T. D. Anthopoulos, J. R. Durrant, C. K. Williams and I. McCulloch, *J. Mater. Chem.*, 2011, **21**, 18744-18752.
- 45 J.-H. Kim, J. B. Park, F. Xu, D. Kim, J. Kwak, A. C. Grimsdale and D.-H. Hwang, *Energy Environ. Sci.*, 2014, **7**, 4118-4131.
- 46 J. Warnan, A. El Labban, C. Cabanetos, E. T. Hoke, P. K. Shukla, C. Risko, J.-L. Brédas, M. D. McGehee and P. M. Beaujuge, *Chem. Mater.*, 2014, **26**, 2299-2306.
- 47 J. W. Jung, T. P. Russell and W. H. Jo, *ACS Appl. Mater. Interf.*, 2015, **7**, 13666-13674.
- 48 M. A. Uddin, T. Kim, S. Yum, H. Choi, S. Hwang, J. Y. Kim and H. Y. Woo, *Curr. Appl. Phys.*, 2015, **15**, 654-661.
- 49 H.-Y. Chen, J. Hou, S. Zhang, Y. Liang, G. Yang, Y. Yang, L. Yu, Y. Wu and G. Li, *Nature Photon.*, 2009, **3**, 649-653.
- 50 Y. Liang, Z. Xu, J. Xia, S.-T. Tsai, Y. Wu, G. Li, C. Ray and L. Yu, *Adv. Mater.*, 2010, **22**, E135-E138.
- 51 L. Dou, J. You, J. Yang, C.-C. Chen, Y. He, S. Murase, T. Moriarty, K. Emery, G. Li and Y. Yang, *Nature Photon.*, 2012, **6**, 180-185.
- 52 Z. Zhang, B. Peng, B. Liu, C. Pan, Y. Li, Y. He, K. Zhou and Y. Zou, *Polym. Chem.*, 2010, **1**, 1441-1447.
- 53 J. Min, Z.-G. Zhang, S. Zhang, M. Zhang, J. Zhang and Y. Li, *Macromolecules*, 2011, **44**, 7632-7638.
- 54 S. C. Price, A. C. Stuart, L. Yang, H. Zhou and W. Yu, *J. Am. Chem. Soc.*, 2011, **133**, 4625-4631.
- 55 D. Kotowski, S. Luzzati, G. Bianchi, A. Calabrese, A. Pellegrino, R. Po, G. Schimperia and A. Tacca, *J. Mater. Chem. A*, 2013, **1**, 10736-10744.
- 56 J. Ku, S. Song, S. H. Park, K. Lee, H. Suh, Y. Lansac and Y. H. Jang, *J. Phys. Chem. C*, 2015, **119**, 14063-14075.
- 57 N. I. Abdo, J. Ku, A. A. El-Shehawey, H.-S. Shim, J.-K. Min, A. A. El-Barbary, Y. H. Jang and J.-K. Lee, *J. Mater. Chem. A*, 2013, **1**, 10306-10317.
- 58 Schrodinger, LLC, New York, NY, version 6.5 edn., 2005.
- 59 B. H. Greeley, T. V. Russo, D. T. Mainz, R. A. Friesner, J.-M. Langlois, W. A. Goddard, III, R. E. Donnelly, Jr. and M. N. Ringalda, *J. Chem. Phys.*, 1994, **101**, 4028-4041.
- 60 M. J. Frisch, G. W. Trucks, H. B. Schlegel, G. E. Scuseria, M. A. Robb, F. R. Cheeseman, J. A. F. Montgomery, T. Vreven, K. N. Kudin, J. C. Burant, F. M. Millam, S. S. Iyengar, F. Tomasi, V. Barone, B. Mennucci,

- M. Cossi, G. Scalmani, N. Rega, G. A. Petersson, G. Nakatsuji, M. Hada, M. Ehara, K. Toyota, R. Fukuda, J. Hasegawa, M. Ishida, T. Nakajima, Y. Honda, O. Kitao, G. Nakai, M. Klene, X. Li, J. E. Know, G. P. Hratchian, J. B. Cross, V. Bakken, C. Adamo, F. Jaramillo, R. Gomperts, R. E. Stratmann, O. Yazyev, A. J. Austin, R. Cmmi, C. Pomelli, J. W. Ochterski, P. Y. Ayala, K. Morokuma, G. A. Voth, P. Salvador, J. J. Dnnenberg, V. G. Zakrzewski, S. Dapprich, A. D. Daniels, M. C. Strain, O. Farkas, D. K. Malick, A. D. Rabuck, R. K., J. B. Foresman, J. V. Ortiz, Q. Cui, A. G. Baboul, S. Cliffoord, J. Coislowski, B. B. Stefanov, G. Liu, A. Iliashenko, P. Piskorz, I. Komaromi, R. L. Martin, D. J. Fox, T. Keith, M. A. Al-Laham, C. Y. Peng, A. Nanayakkara, M. Challacombe, P. M. W. Gill, B. Jognson, W. Chen, M. W. Wong, C. Gonzalez and J. A. Pople, Gaussian, Inc., Wallingford, CT, Revision C.02 edn., 2004.
- 61 J. C. Slater, *Quantum Theory of Molecules and Solids. Vol. 4. The Self-Consistent Field for Molecules and Solids*, McGraw-Hill, New York, 1974.
- 62 A. D. Becke, *Phys. Rev. A*, 1988, **38**, 3098-3100.
- 63 S. H. Vosko, L. Wilk and M. Nusair, *Can. J. Phys.*, 1980, **58**, 1200-1211.
- 64 C. Lee, W. Yang and R. G. Parr, *Phys. Rev. B*, 1988, **37**, 785-789.
- 65 B. Miehlich, A. Savin, H. Stoll and H. Preuss, *Chem. Phys. Lett.*, 1989, **157**, 200-206.
- 66 V. Barone and M. Cossi, *J. Phys. Chem. A*, 1998, **102**, 1995-2001.
- 67 M. Cossi, N. Rega, G. Scalmani and V. Barone, *J. Comput. Chem.*, 2003, **24**, 669-681.
- 68 L. Pandey, C. Risko, J. E. Norton and J.-L. Brédas, *Macromolecules*, 2012, **45**, 6405-6414.
- 69 E. Runge and E. K. U. Gross, *Phys. Rev. Lett.*, 1984, **52**, 997-1000.
- 70 R. E. Stratmann, G. E. Scuseria and M. J. Frisch, *J. Chem. Phys.*, 1998, **109**, 8218-8224.
- 71 M. E. Casida, C. Jamorski, K. C. Casida and D. R. Salahub, *J. Chem. Phys.*, 1998, **108**, 4439-4449.
- 72 K. Burke, J. Werschnik and E. K. U. Gross, *J. Chem. Phys.*, 2005, **123**, 062206.
- 73 A. D. Becke, *J. Chem. Phys.*, 1997, **107**, 8554-8560.
- 74 J.-D. Chai and M. Head-Gordon, *J. Chem. Phys.*, 2008, **128**, 084106.
- 75 J.-D. Chai and M. Head-Gordon, *Phys. Chem. Chem. Phys.*, 2008, **10**, 6615-6620.
- 76 S. Grimme, *J. Comput. Chem.*, 2004, **25**, 1463-1473.
- 77 S. Grimme, *J. Comput. Chem.*, 2006, **27**, 1787-1799.
- 78 K. E. Riley, M. Pitonak, P. Jurecka and P. Hobza, *Chem. Rev.*, 2010, **110**, 5023-5063.
- 79 K. W. Song, M. H. Choi, J. Y. Lee and D. K. Moon, *J. Ind. Eng. Chem.*, 2014, **20**, 290-296.
- 80 X. Liu, R. He, W. Shen and M. Li, *J. Power Sources*, 2014, **245**, 217-223.
- 81 M. Koppe, H.-J. Egelhaaf, G. Dennler, M. C. Scharber, C. J. Brabec, P. Schilinsky and C. N. Hoth, *Adv. Funct. Mater.*, 2010, **20**, 338-346.
- 82 M. C. Scharber, M. Koppe, J. Gao, F. Cordella, M. A. Loi, P. Denk, M. Morana, H.-J. Egelhaaf, K. Forberich, G. Dennler, R. Gaudiana, D. Waller, Z. Zhu, X. Shi and C. J. Brabec, *Adv. Mater.*, 2010, **22**, 367-370.
- 83 C. M. Cardona, W. Li, A. E. Kaifer, D. Stockdale and G. C. Bazan, *Adv. Mater.*, 2011, **23**, 2367-2371.
- 84 L. E. Polander, L. Pandey, S. Barlow, S. P. Tiwari, C. Risko, B. Kippelen, J.-L. Brédas and S. R. Marder, *J. Phys. Chem. C*, 2011, **115**, 23149-23163.
- 85 A. B. Koren, M. D. Curtis and J. W. Kampf, *Chem. Mater.*, 2000, **12**, 1519-1522.
- 86 C. Soci, I. W. Hwang, D. Moses, Z. Zhu, D. Waller, R. Gaudiana, C. J. Brabec and A. J. Heeger, *Adv. Funct. Mater.*, 2007, **17**, 632-636.
- 87 M. Zhang, H. N. Tsao, W. Pisula, C. Yang, A. K. Mishra and K. Mullen, *J. Am. Chem. Soc.*, 2007, **129**, 3472-3473.
- 88 H.-Y. Chen, J. Hou, A. E. Hayden, H. Yang, K. N. Houk and Y. Yang, *Adv. Mater.*, 2010, **22**, 371-375.
- 89 M. Tong, S. Cho, J. T. Rogers, K. Schmidt, B. B. Y. Hsu, D. Moses, R. C. Coffin, E. J. Kramer, G. C. Bazan and A. J. Heeger, *Adv. Funct. Mater.*, 2010, **20**, 3959-3965.
- 90 P. M. Beaujuge, C. M. Amb and J. R. Reynolds, *Acc. Chem. Res.*, 2010, **43**, 1396-1407.
- 91 E. Iizuka, M. Wakioka and F. Ozawa, *Macromolecules*, 2015, **48**, 2989-2993.
- 92 M. C. Scharber, D. Muhlbacher, M. Koppe, P. Denk, C. Waldauf, A. J. Heeger and C. J. Brabec, *Adv. Mater.*, 2006, **18**, 789-794.
- 93 N. Blouin, A. Michaud, D. Gendron, S. Wakim, E. Blair, R. Neagu-Plesu, M. Belletete, G. Durocher, Y. Tao and M. Leclerc, *J. Am. Chem. Soc.*, 2008, **130**, 732-742.
- 94 N. Berube, V. Gosselin, J. Gaudreau and M. Cote, *J. Phys. Chem. C*, 2013, **117**, 7964-7972.
- 95 J. K. Lee, W. L. Ma, C. J. Brabec, J. Yuen, J. S. Moon, J. Y. Kim, K. Lee, G. C. Bazan and A. J. Heeger, *J. Am. Chem. Soc.*, 2008, **130**, 3619-3623.
- 96 J. Peet, M. L. Senatore, A. J. Heeger and G. C. Bazan, *Adv. Mater.*, 2009, **21**, 1521-1527.
- 97 J.-L. Brédas, D. Beljonne, V. Coropceanu and J. Cornil, *Chem. Rev.*, 2004, **104**, 4971-5003.
- 98 H. Liu, J. Mu and J. Y. Lee, *J. Phys. Chem. B*, 2011, **115**, 8409-8416.
- 99 J. D. Azoulay, Z. A. Koretz, B. M. Wong and G. C. Bazan, *Macromolecules*, 2013, **46**, 1337-1342.
- 100 Z. Fei, X. Gao, J. Smith, P. Pattanasattayavong, E. B. Domingo, N. Stingelin, S. E. Watkins, T. D. Anthopoulos, R. J. Kline and M. Heeney, *Chem. Mater.*, 2013, **25**, 59-68.
- 101 Z.-L. Cai, K. Sendt and J. R. Reimers, *J. Chem. Phys.*, 2002, **117**, 5543-5549.
- 102 A. Dreuw and M. Head-Gordon, *J. Am. Chem. Soc.*, 2004, **126**, 4007-4016.
- 103 L. Pandey, C. Doiron, J. S. Sears and J.-L. Brédas, *Phys. Chem. Chem. Phys.*, 2012, **14**, 14243-14248.
- 104 H. Iikura, T. Tsuneda, T. Yanai and K. Hirao, *J. Chem. Phys.*, 2001, **115**, 3540-3544.
- 105 T. Yanai, D. P. Tew and N. C. Handy, *Chem. Phys. Lett.*, 2004, **393**, 51-57.
- 106 T. M. McCormick, C. R. Bridges, E. I. Carrera, P. M. DiCarmine, G. L. Gibson, J. Hollinger, L. M. Kozycz and D. S. Seferos, *Macromolecules*, 2013, **46**, 3879-3886.
- 107 S. B. Li, Y.-A. Duan, Y. Geng, H.-B. Li, J. Z. Zhang, H. L. Xu, M. Zhang and Z.-M. Su, *Phys. Chem. Chem. Phys.*, 2014, **16**, 25799-25808.